V. V. Zlobin, A. A. Krasilin, O. V. Almjasheva, Effect of heterogeneous inclusions on the formation of TiO_2 nanocrystals in hydrothermal conditions,
Nanosystems: Physics, Chemistry, Mathematics, 2019, Volume 10, Issue 6, 733–739

NANOSYSTEMS: PHYSICS, CHEMISTRY, MATHEMATICS, 2019, 10 (6), P. 733–739

Effect of heterogeneous inclusions on the formation of TiO_2 nanocrystals in hydrothermal conditions

V. V. Zlobin[1], A. A. Krasilin[2], O. V. Almjasheva[1,2]

[1]Saint Petersburg Electrotechnical University "LETI", Professor Popov St. 5, Saint Petersburg, 197376, Russia
[2]Ioffe Institute, Politekhnicheskaya St. 26, Saint Petersburg, 194021, Russia

zvv1210@yandex.ru, ikrasilin@mail.ioffe.ru, almjasheva@mail.ru

PACS 81.07.Wx **DOI 10.17586/2220-8054-2019-10-6-733-739**

The effects of heterogeneous impurities on the process of titanium dioxide nanoparticle formation during hydrothermal synthesis and photocatalytic properties of synthesized particles were studied. Pre-formed TiO_2 nanoparticles of anatase and rutile modifications were used as the heterogeneous impurity. It is shown that the heterogeneous impurities may be considered neither as geometric constraints precluding the crystallization, nor as crystallization centers.

Keywords: nanoparticles, titanium dioxide, anatase, rutile, hydrothermal synthesis.

Received: 24 September 2019

Revised: 18 November 2019

1. Introduction

Currently, titanium dioxide is of significant interest, both as an object of fundamental research [1–4] and material for various practical applications [5–23]. Nanosized powders of titanium dioxide are used in metallurgy [5, 6], electronics [7–9], polymer industry [10, 11], photovoltaics [12–15], and biomedicine [16, 17]. Another important area for nanocrystalline titanium dioxide is photocatalysis [13, 18–23]. Since the properties of TiO_2 nanoparticles strongly depend on phase composition, morphology and surface structure, many scientific papers focus on formation mechanism and design of various titanium oxide nanocrystals [1, 18–29].

Despite great number of papers on the effect of formation conditions on the obtained structure and properties of titanium dioxide nanoparticles, there is still uncertainty in the mechanisms of various modifications formation and their stability ranges. The thermodynamically stable TiO_2 modification (for macro-sized particles) is that with rutile structure. However, nanocrystals of titanium dioxide anatase modification are predominantly formed as a result of the soft chemistry synthesis [1, 4, 18, 24, 26, 28–31]. The transformation of anatase into rutile only takes place upon additional thermal treatment accompanied by crystal growth [32–35].

It is also unclear, which TiO_2 modification is the most active photocatalyst, how an amorphous component influences the catalytic properties of titanium oxide, which ratio of the amorphous and different crystalline phases is to be chosen for maximum catalytic activity [22, 26, 29, 30, 35–37].

The studies [38–40] demonstrated that the structural and morphological characteristics of nanoparticles being formed may be changed by introducing a heterogeneous impurity to act either as geometrical constraints or as crystal-nucleating centers providing the phases' structural continuity. Therefore, it is of interest to study the effect of a heterogeneous impurity on the process of titanium dioxide nanoparticles formation during hydrothermal synthesis and also on the particles' photocatalytic properties.

2. Experimental section

Pre-formed nanocrystalline titanium dioxide particles of rutile and anatase structure were used as the nanosized particles introduced into the reaction medium during nanocrystalline TiO_2 synthesis.

The titanium dioxide nanocrystals of rutile and anatase structure were obtained under hydrothermal conditions by dehydration of hydrated titanium dioxide ($TiO_2 \cdot nH_2O$) derivedby precipitation from a dilute solution of titanium tetrachloride (high pure 12-3, TU 6-09-2118-77) using an ammonium hydroxide solution (reagent-grade, GOST 3760-79).

The effect of impurity phases on the titanium dioxide crystallization process was studied by precipitating $TiO_2 \cdot nH_2O$ from $TiCl_4$ dilute solution in a suspension of pre-formed titanium dioxide nanoparticles of various structures, using ammonium hydroxide solution, with subsequent hydrothermal treatment.

The hydrothermal treatment was conducted at 250 °C and $P = 70$ MPa. PTFE liners with the reagents were placed into steel autoclaves and loaded into an oven. Upon completion of isothermal exposure at specified temperatures, the oven was switched off, and the autoclaves and the oven were left to cool. The accuracy of the isothermal exposure temperature control was $\pm 5^{\circ}$. The hydrothermal treatment time was recorded by duration of the autoclaves' isothermal exposure in the oven. The synthesis products were rinsed with distilled water and dried at a temperature of 90 °C. The duration of the hydrothermal treatment at the oven temperature of 250 °C varied from 15 min to 4 hours. Distilled water was used as the hydrothermal fluid.

To determine the samples' elemental composition, we carried out energy dispersive X-ray spectroscopy (EDS) on FEI Quanta 200 scanning electron microscope with EDAX analyzer.

The phase analysis was carried out by x-ray diffraction, using Rigaku Smart Lab 3 X-ray powder diffractometer. The phase identification was performed by comparing the obtained diffractograms with ICDD database cards. The rutile to anatase ratio was calculated by formula proposed in [41]. The crystallites' dimensions were assessed by X-ray diffraction line broadening, using Scherrer formula. The crystallite size distribution was determined by XRD profile analysis, with the use of Rigaku Smart Lab 3 and Maud software packages.

Photocatalytic activity of the obtained compositions was studied under HPX-2000-HP-DUV xenon source radiation with a nominal power of 75 W. The weighed sample powder was dispersed in distilled water with ultrasonication during 30 minutes. Then 1.9 ml of the suspension was transferred into a standard PMMA cell which then was placed into a spectrometer compartment. The cell content was mixed throughout the experiment using a magnetic stirrer and thermally controlled at 25 °C. 75 μl of 400 mg/l crystal violet water solution was added to the suspension. The obtained mixture was held for 30 min in a dark place to take account of the possible dye adsorption, and then irradiated for 2 hours. The change in the dye concentration was calculated by reduction in the absorption peak intensity. Commercial titanium dioxide Degussa P25 powder was used as reference material.

3. Results and discussion

The titanium dioxide nanoparticles pre-formed in hydrothermal conditions were TiO_2 of rutile (Fig. 1, curve *1*) and anatase (Fig. 1, curve *2*) structure with a crystallite size of about 10 and 15 nm, respectively. Based on the XRD line nature of the TiO_2 rutile sample (Fig. 1, curve *1*), it can be concluded that a part of titanium dioxide is in X-ray amorphous state.

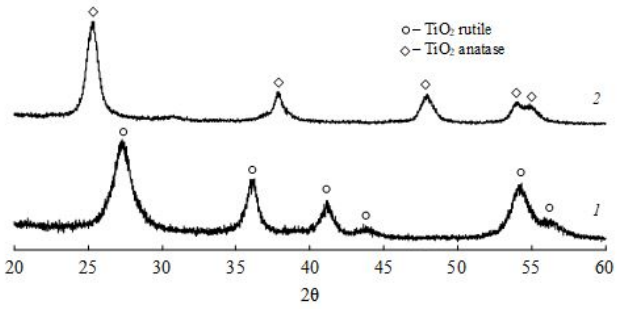

FIG. 1. X-ray diffractograms of the pre-formed nanocrystals: *1* – TiO_2 (rutile); *2* – TiO_2 (anatase)

According to X-ray diffraction data, the samples' X-ray diffractograms obtained after hydrated titanium dioxide precipitation in the suspension of nanoparticles demonstrated X-ray peaks corresponding to TiO_2 crystalline phases, in the suspension of which the hydrated titanium dioxide precipitation was carried out (Fig. 2, curves *1* and *2*).

For the reference material, hydrated titanium dioxide was used, which was obtained by precipitating from titanium tetrachloride dilute solution, in accordance with a method identical to that for obtaining the compositions. The X-ray diffractogram shown in Fig. 2, curve *1*, indicates that $TiO_2 \cdot nH_2O$ obtained as a result of the precipitation is in X-ray amorphous state. Based on the data of X-ray diffraction analysis of hydrated titanium dioxide obtained by precipitation with no impurities and of $TiO_2 \cdot nH_2O$ precipitated in the suspension of TiO_2 nanoparticles of various modifications (curve *1* and curves *2* and *3*, respectively), it can be supposed that the latter is likely to be not all-crystalline and that a part of the substance is likely to be in X-ray amorphous state. Based on the elemental analysis data, it can be concluded that impurity elements, the presence of which may arise out of the precipitation method, such as Cl^- ions, are absent.

Figure 3 shows x-ray diffractograms for the samples obtained as a result of hydrothermal treatment at 250 °C for 0.5 h, as an example.

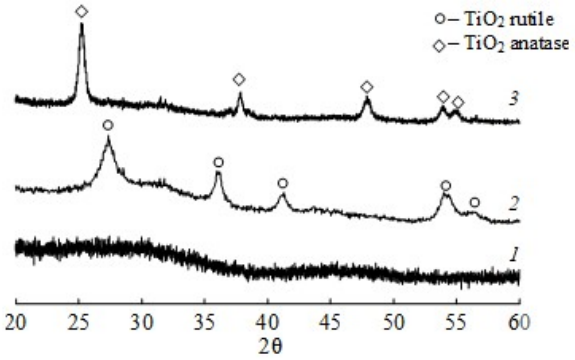

FIG. 2. X-ray diffractograms of the initial compositions: *1* – $TiO_2 \cdot nH_2O$; *2* – TiO_2(rutile)–$TiO_2 \cdot nH_2O$; *3* – TiO_2(anatase)–$TiO_2 \cdot nH_2O$

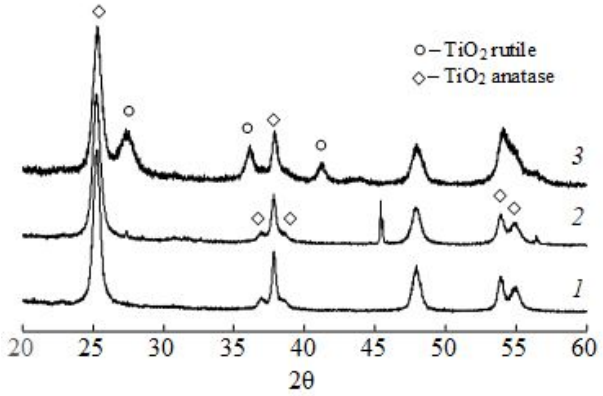

FIG. 3. X-ray diffractograms for the samples obtained as a result of hydrothermal treatment at 250 °C for 0.5 h. *1* – $TiO_2 \cdot nH_2O$; *2* – TiO_2(anatase)–$TiO_2 \cdot nH_2O$; *3* – TiO_2(rutile)–$TiO_2 \cdot nH_2O$

The X-ray diffractograms both of the samples with no heterogeneous impurity (Fig. 3, curve *1*) and of the samples obtained by precipitation in the suspension of titanium oxide nanoparticles of various structural modifications, after hydrothermal treatment (Fig. 3, curves *2* and *3*) demonstrated X-ray peaks corresponding to TiO_2 anatase modification. The increase in the isothermal exposure period for all the samples led to increased intensity of anatase peaks, however, for the system TiO_2(rutile)–$TiO_2 \cdot nH_2O$, the intensity of reflexes corresponding to TiO_2-rutile only changed insignificantly. Only reduction in the X-ray peak broadening was observed, which may indicate increase in the crystallite dimensions.

Based on the X-ray diffraction data, crystallization degrees and crystallite dimensions were plotted against the duration of isothermal exposure (Fig. 4–5).

As it is seen from Fig. 4, at the hydrothermal treatment initial stage, during the first 30 minutes, a rather intensive anatase formation is observed: the anatase fraction in the system increases from 0.2 to ~ 0.75 mol.%. This can likely be explained by TiO_2 (anatase) particle crystallization from the amorphous phase. In this case, the nature of change in the crystalline modification fraction corresponds to that of crystallization of titanium dioxide with no impurities. The size of crystallites of titanium dioxide formed is systematically smaller than that of crystallites in the system TiO_2(anatase)–$TiO_2 \cdot nH_2O$. Moreover, the dependence between the size of titanium dioxide crystallites obtained with no heterogeneous impurities and the isothermal exposure duration is monotonic. While in the system "TiO_2(anatase)–$TiO_2 \cdot nH_2O$", the initial stage of crystallization is accompanied by reduction in the mean size of anatase crystallites (Fig. 4(b), curve *2*). It is likely that in the case of crystallization from the amorphous phase the size of particles formed is much smaller than that of anatase particles already introduced as the heterogeneous impurity (see Fig. 4(b), curve *1*), which leads to a reduction in the crystallite mean size. During the subsequent hydrothermal treatment of the reaction system, phase formation mechanism is changed, which leads to slowing down of the crystallization rate. And the anatase crystallite growth is due to the processes of crystallization of the remaining amorphous phase on the

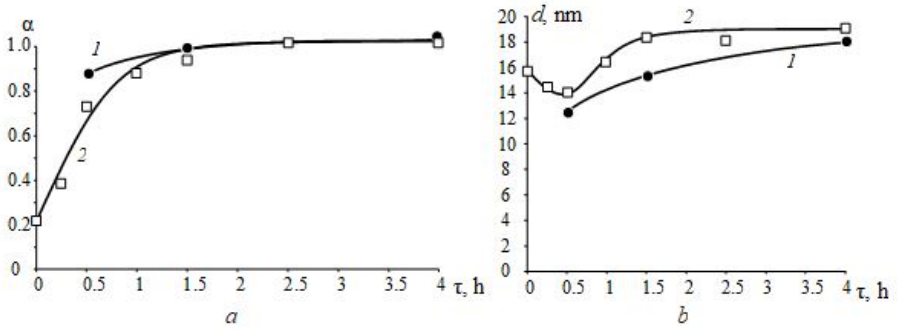

FIG. 4. Crystalline phase (TiO_2-anatase) fraction (a) and anatase crystallite dimensions (b) as a function of the duration of $TiO_2 \cdot nH_2O$ hydrothermal treatment (curves *1*) and of the composition of TiO_2(anatase)–$TiO_2 \cdot nH_2O$ (curves *2*)

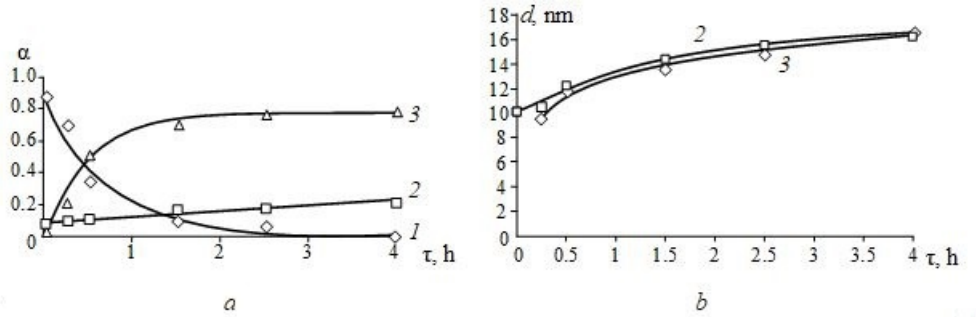

FIG. 5. Amorphous and crystalline phase (TiO_2-anatase, rutile) fraction (a) and anatase crystallite mean size (b) as a function of the duration of the composition TiO_2(rutile)–$TiO_2 \cdot nH_2O$ hydrothermal treatment at a temperature of 250 °C: *1* – amorphous fraction; *2* – TiO_2 with rutile structure; *3* – TiO_2 with anatase structure

anatase particles surface, which, in its turn, leads to systematically larger crystallite sizes in the system TiO_2(anatase)–$TiO_2 \cdot nH_2O$ as compared to crystallites formed as a result of hydrothermal treatment of $TiO_2 \cdot nH_2O$.

As a result of hydrothermal treatment of the composition obtained by precipitating $TiO_2 \cdot nH_2O$ in the suspension of rutile nanoparticles, peaks corresponding to anatase structure titanium dioxide appear in the X-ray diffractograms (Fig. 3, curve *3*). Increase in the hydrothermal treatment duration leads to increased anatase peak intensity. However, increase in the fraction of rutile structure TiO_2 phase is very insignificant (Fig. 5(a)).

From the relationship of anatase crystalline phase fraction and change in the mean size of anatase crystallites formed as a result of hydrothermal treatment (Fig. 5) and also the data of TiO_2 crystallization process analysis shown in Fig. 4(a), curve *1*, it is seen that in this case, anatase is also formed at the initial stage from the amorphous phase due to the process of nucleation. And, judging by mild correlation with the change in the fraction of crystalline titanium dioxide with rutile structure, the X-ray amorphous component probably contained in the heterogeneous impurity (Fig. 1, curve *2*) is also crystallized primarily as anatase structural modification.

Thus, it can be concluded that the use of a heterogeneous impurity of the studied composition and particle size has almost no effect on the process of phase formation in the TiO_2–H_2O system. This is likely due to the fact that the distance between the introduced nanoparticles significantly exceeds the size of TiO_2 critical nucleus [42]. Thus, the heterogeneous impurities may be considered neither as geometric constraints precluding the crystallization, as it was the case for Al_2O_3 [39, 43] or Cr_2O_3 [44], nor as crystallization centers.

On the one hand, the absence of any effect of titanium dioxide nanoparticles of various structural modifications on the phase composition of $TiO_2 \cdot nH_2O$ formed as a result of dehydration under hydrothermal conditions may be associated with significant difference in the sizes of titanium dioxide critical nucleus and of crystallites introduced as the heterogeneous impurity. On the other hand, clusters are likely to be formed during the precipitation of $TiO_2 \cdot nH_2O$ from the titanium tetrachloride solution, and the arrangement of titanium and oxygen atoms in the clusters is similar to anatase structural elements [43, 44]. And at the hydrothermal treatment stage, the anatase-like clusters grow together following the accommodative mechanism, as it was proposed in [43].

The results of photocatalytic properties assessment for samples synthesized by hydrothermal treatment of compositions obtained by $TiO_2 \cdot nH_2O$ precipitation in the suspension of anatase and rutile nanoparticles are presented in Fig. 6.

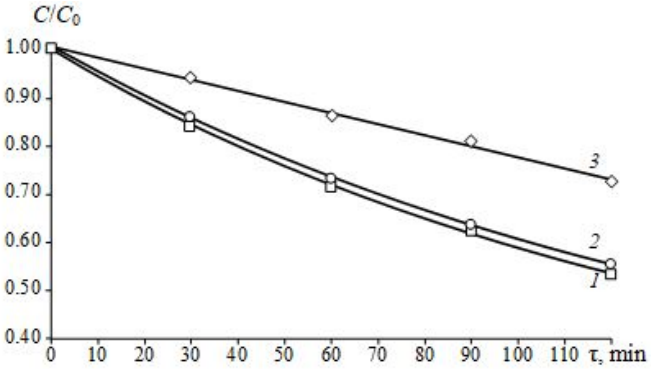

FIG. 6. Coloring agent relative concentration change as a function of UV-exposure time: *1* – commercial material TiO_2 (P25 Degussa), *2* – sample obtained by hydrothermal treatment of TiO_2(anatase)–$TiO_2 \cdot nH_2O$, *3* – sample obtained by hydrothermal treatment of TiO_2(rutile)–$TiO_2 \cdot nH_2O$

The analysis of relationships presented in Fig. 6 allows concluding that the sample composed only of the anatase modification (Fig. 6, curve *2*) demonstrates characteristics comparable to that of the commercial material (Fig. 6, curve *1*). While even an insignificant quantity of rutile titanium dioxide leads to remarkable reduction in the system photocatalytic activity (Fig. 6, curve *3*). On one hand, the results agree with literature data, e.g., [26, 45], indicating that the anatase modification of titanium dioxide exhibits higher catalytic properties than rutile one. However, the reference material P25 Degussa that, according to [36], consists of a mixture of anatase, rutile and in some cases amorphous TiO_2, demonstrates almost equal photocatalytic properties than the anatase sample. Based on the obtained results, it can be supposed that the determining influence on titanium dioxide photocatalytic activity is produced by an interface between various TiO_2 modifications formed during the material synthesis. In case of the precipitation method used, the particles of anatase and rutile are likely to be in pinpoint contact that has no effect on the obtained system properties, and the method for obtaining P25 Degussa, i.e. pyrolysis of titanium tetrachloride, allows for more active superficial contact of anatase and rutile.

4. Conclusions

Thus, based on the obtained data, it can be concluded that to control the formation process of titanium dioxide of any structural modification, we need to vary the conditions of $TiO_2 \cdot nH_2O$ precipitation from the solution, alter the chemical composition of precursors [25, 27–31], or precipitation procedures [47, 48].

Acknowledgements

The authors express their gratitude to V. V. Gusarov for the attention he paid to the work. X-ray diffraction was performed using the equipment of the Engineering Center Saint Petersburg State Institute of Technology. This study was financially supported by the Russian Science Foundation (project No. 16-13-10252).

References

[1] Savinkina E.V., Kuz'micheva G.M., et al. Synthesis and morphology of anatase and η-TiO_2 nanoparticles. *Inorganic Materials*, 2011, **47** (5), P. 489–494.

[2] Hanaor D.A.H. Sorrell C.C. Review of the anatase to rutile phase transformation. *Journal of Materials Science*, 2011, **46** (4), P. 855–874.

[3] Esmaeilzadeh J., Ghashghaie S., et al. Effect of dispersant on chain formation capability of TiO_2 nanoparticles under low frequency electric fields for NO_2 gas sensing applications. *Journal of the European Ceramic Society*, 2014, **34** (5), P. 1201–1208.

[4] Rahiminezhad-Soltani M., Saberyan K., Shahri F., Simchi A. Formation mechanism of TiO_2 nanoparticles in H_2O-assisted atmospheric pressure CVS process. *Powder Technology*, 2011, **209** (1–3), P. 15–24.

[5] Kumar C.A.V., Rajadurai J.S. Influence of rutile (TiO_2) content on wear and microhardness characteristics of aluminium-based hybrid composites synthesized by powder metallurgy. *Transactions of Nonferrous Metals Society of China*, 2016, **26** (1), P. 63–73.

[6] Chougule A.B., Patil P.M., Umasankar V. Enhancement of hardness property of AA2219 by varying TiO_2 percentage as a reinforcement. *Materials Today: Proceedings*, 2018, **5** (2, Part 2), P. 7628–7634.

[7] Lü X., Yang W., et al. Enhanced electron transport in Nb-doped TiO_2 nanoparticles via pressure-Induced phase transitions. *Journal of the American Chemical Society*, 2014, **136** (1), P. 419–426.
[8] Huang Y., Zhang J. The electrical behaviors of anatase titanium dioxide (TiO_2) nanoparticles under high pressure. *Solid State Communications*, 2019, **287**, P. 1–6.
[9] Shen L., Zhang X., et al. Design and tailoring of a three dimensional TiO_2-graphene-carbon nanotube nanocomposite for fast lithium storage. *The Journal of Physical Chemistry Letters*, 2011, **2** (24), 3096.
[10] Tian C. Internal influences of hydrolysis conditions on rutile TiO_2 pigment production via short sulfate process. *Materials Research Bulletin*, 2018, **103**, P. 83–88.
[11] Sun M., Liu F., Shi H. Han E. A study on water absorption in freestanding polyurethane films filled with nano-TiO_2 pigments by capacitance measurements. *Acta Metallurgica Sinica (English Letters)*, 2009, **22** (1), P. 27–34.
[12] Vildanova M.F., Kozlov S.S., et al. Niobium-doped titanium dioxide nanoparticles for electron transport layers in perovskite solar cells. *Nanosystems: Physics, Chemistry, Mathematics*, 2017, **8** (4), P. 540–545.
[13] Haffad S., Kiprono K.K. Interfacial structure and electronic properties of TiO_2/ZnO/TiO_2 for photocatalytic and photovoltaic applications: A theoretical study. *Surface Science*, 2019, **686**, P. 10–16.
[14] Wan J., Tao L., et al. A facile method to produce TiO_2 nanorods for high-efficiency dye solar cells. *Journal of Power Sources*, 2019, **438**, 227012.
[15] Marandi M., Goudarzi Z., Moradi L. Synthesis of randomly directed inclined TiO_2 nanorods on the nanocrystalline TiO_2 layers and their optimized application in dye sensitized solar cells. *Journal of Alloys and Compounds*, 2017, **711**, P. 603–610.
[16] Lamberti A., Pirri C.F. TiO_2 nanotube array as biocompatible electrode in view of implantable supercapacitors. *Journal of Energy Storage*, 2016, **8**, P. 193–197.
[17] Katahira K., Mifune N., Komotori J. Generation of biocompatible TiO_2 layer using atmospheric pressure plasma-assisted fine particle peening. *CIRP Annals*, 2017. **66** (1), P. 515–518.
[18] Kolen'ko Y.V., Garshev A.V., et al. Photocatalytic activity of sol-gel derived titania converted into nanocrystalline powders by supercritical drying. *Journal of Photochemistry and Photobiology A: Chemistry*, 2005, **172**, P. 19–26.
[19] Cabrera-Reina A., Martínez-Piernas A.B., et al. TiO_2 photocatalysis under natural solar radiation for the degradation of the carbapenem antibiotics imipenem and meropenem in aqueous solutions at pilot plant scale. *Water Research*, 2019, **166**, 115037.
[20] Vorontsov, A.V., Kozlov, D. V., Smirniotis, P. G., Parmon, V. N. TiO_2 photocatalytic oxidation: II. Gas-phase processes. *Kinetics and Catalysis*, 2005, **46** (3), P. 422–436.
[21] Humayun M., Raziq F., Khan A., Luo W. Modification strategies of TiO_2 for potential applications in photocatalysis: a critical review. *Green Chemistry Letters and Reviews*, 2018, **11** (2), P. 86–102.
[22] Savinkina E.V., Obolenskaya L.N., et al. A new η-itania-based photocatalyst. *Doklady Physical Chemistry*, 2011, **441** (1), P. 224–226.
[23] Savinkina E.V., Obolenskaya L.N., et al. Effects of peroxo precursors and annealing temperature on properties and photocatalytic activity of nanoscale titania. *Journal of Materials Research*, 2018, **33** (10), P. 1422–1432.
[24] Rahiminezhad-Soltani M., Saberyan K., Shahri F., Simchi A. Formation mechanism of TiO_2 nanoparticles in H_2O-assisted atmospheric pressure CVS process. *Powder Technology*, 2011, **209** (1–3), P. 15–24.
[25] Machida M, Kobayashi M., Suzuki Y., Abe H. Facile synthesis of $>$ 99 % phase-pure brookite TiO_2 by hydrothermal conversion from Mg_2TiO_4. *Ceramics International*, 2018. **44** (14), P. 17562–17565.
[26] Allen N.S., Mahdjoub N., et al. The effect of crystalline phase (anatase, brookite and rutile) and size on the photocatalytic activity of calcined polymorphic titanium dioxide (TiO_2). *Polymer Degradation and Stability*, 2018, **150**, P. 31–36.
[27] Leal J.H., Cantu Y., Gonzalez D.F., Parsons J.G. Brookite and anatase nanomaterial polymorphs of TiO_2 synthesized from $TiCl_3$. *Inorganic Chemistry Communications*, 2017, **84**, P. 28–32.
[28] de Mendona V.R., Lopes O.F., et al. Insights into formation of anatase TiO_2 nanoparticles from peroxo titanium complex degradation under microwave-assisted hydrothermal treatment. *Ceramics International*, 2019, **45** (17, Part B), P. 22998–23006.
[29] Macwan D.P., Dave P.N., Chaturvedi S. A review on nano-TiO_2 sol–gel type syntheses and its applications. *Journal of Materials Science*, 2011, **46** (11), P. 3669–3686.
[30] Kaifeng Yu K., Ling M., Liang J., Liang C. Formation of TiO_2 hollow spheres through nanoscale Kirkendall effect and their lithium storage and photocatalytic properties. *Chemical Physics*, 2019, **517**, P. 222–227.
[31] Wang C.-C., Ying J.Y. Sol-gel synthesis and hydrothermal processing of anatase and rutile titania nanocrystals. *Chemistry of Materials*, 1999, **11** (19), P. 3113–3120.
[32] Ding X.-Z., Liu X.-H. Correlation between anatase-to-rutile transformation and grain growth in nanocrystalline titania powders. *Journal of Materials Research*, 1998, **13** (9), P. 2556–2559.
[33] Gribb A.A., Banfield J.F. Particle size effects on transformation kinetics and phase stability in nanocrystalline TiO_2. *American Mineralogist*, 1997, **82**, P. 717–728.
[34] Yang J., Gao M., et al. Hysteretic phase transformation of two-dimensional TiO_2. *Materials Letters*, 2018, **232**, P. 171–174.
[35] Wang Y., Zhang W., et al. Fabrication of TiO_2(B)/anatase heterophase junctions in nanowires *via* a surface-preferred phase transformation process for enhanced photocatalytic activity. *Chinese Journal of Catalysis*, 2018, **39** (9), P. 1500–1510.
[36] Ohtani B., Prieto-Mahaney O.O., Li D., Abe R. What is Degussa (Evonik) P25? Crystalline composition analysis, reconstruction from isolated pure particles and photocatalytic activity test. *Journal of Photochemistry and Photobiology A: Chemistry*, 2010, **216** (2–3), P. 179–182.
[37] Ohno T., Sarukawa K., Matsumura M. Photocatalytic Activities of Pure Rutile Particles Isolated from TiO_2 Powder by Dissolving the Anatase Component in HF Solution. *The Journal of Physical Chemistry B*, 2001, **105**, P. 2417–2420.
[38] Yorov Kh.E., Sipyagina N.A., et al. SiO_2–TiO_2 binary aerogels: Synthesis in new supercritical fluids and study of thermal stability. *Russian Journal of Inorganic Chemistry*, 2016, **61** (11), P. 1339–1346
[39] Almjashev O.V., Gusarov V.V. Effect of ZrO_2 nanocrystals on the stabilization of the amorphous state of alumina and silica in the ZrO_2–Al_2O_3 and ZrO_2–SiO_2 systems. *Glass Physics and Chemistry*, 2006, **32** (2), P. 162–166.
[40] Gusarov V.V. Malkov A.A., Malygin A.A., Suvorov S.A. Formations of aluminum titanate in compositions with a high level of spatial and structural conjugation of components. *Russian Journal of General Chemistry*, 1994, **64** (4), P. 554–557. (in Russian)

[41] Spurr R.A., Myers H. Quantitative Analysis of Anatase-Rutile Mixtures with an X-Ray Diffractometer. *Analytical Chemistry*, 1957, **29** (5), P. 760–762.

[42] Almjasheva O.V. Formation and structural transformations of nanoparticles in the TiO_2–H_2O system. *Nanosystems: Physics, Chemistry, Mathematics*, 2016, **7** (6), P. 1031–1049.

[43] Al'myashev O.V., Gusarov V.V. Features of the phase formation in the nanocomposites. *Russian Journal of General Chemistry*, 2010, **80** (3), P. 385–390

[44] Almjasheva O.V. Formation of oxide nanocrystals and nanocomposites in hydrothermal conditions, structure and properties of materials on their basis. Abstract of dissertation for the degree of Doctor of Sciences, 2018, 44 p. (in Russian)

[45] Almjasheva O.V., Gusarov V.V. Metastable clusters and aggregative nucleation mechanism. *Nanosystems: Physics, Chemistry, Mathematics*, 2014, **5** (3), P. 405–417.

[46] Lebedev V.A., Kozlov D.A., et al. The amorphous phase in titania and its influence on photocatalytic properties. *Applied Catalysis B: Environmental*, 2016, **195**, P. 39–47.

[47] Proskurina O.V., Nogovitsin I.V., et al. Formation of $BiFeO_3$ nanoparticles using impinging jets microreactor. *Russian Journal of General Chemistry*, 2018, **88** (10), P. 2139–2143.

[48] Abiev R.S., Almyasheva O.V., Izotova S.G., Gusarov V.V. Synthesis of cobalt ferrite nanoparticles by means of confined impinging-jets reactors. *Journal of Chemical Technology and Applications*, 2017, **1** (1), P. 7–13.